# Valence Bond Modeling of Barriers in the Nonidentity Hydrogen Abstraction Reactions, $X'\bullet + H-X \rightarrow X'-H + X\bullet$ ($X' \neq X = CH_3$, $SiH_3$, $GeH_3$, $SnH_3$, $PbH_3$)

**Lingchun Song,[†] Wei Wu,*[,†] Kunming Dong,[†] Philippe C. Hiberty,[‡] and Sason Shaik*[,§]**

*Department of Chemistry and State Key Laboratory for Physical Chemistry of Solid Surfaces, Xiamen University, Xiamen, Fujian 361005, P. R. of China, Laboratoire de Chimie physique, Groupe de Chimie Théorique, Université de Paris-Sud, 91405 ORSAY Cédex, France, and Department of Organic Chemistry and the Lise Meitner-Minerva Center for Computational Quantum Chemistry, The Hebrew University, Jerusalem 91904, Israel*

*Received: July 3, 2002; In Final Form: August 29, 2002*

Breathing orbital valence bond (BOVB) computations (Hiberty, P. C.; Humbel, S.; Byrman, C. P.; van Lenthe, J. H. *J. Chem. Phys.* **1994**, *101*, 5969) are used to obtain nonidentity barriers for hydrogen transfer reactions between X and X′ groups, $X \neq X' = CH_3$, $SiH_3$, $GeH_3$, $SnH_3$, $PbH_3$. Modeling of these barriers by means of VB state correlation diagrams (Shaik, S.; Shurki, A. *Angew. Chem., Int. Ed. Engl.* **1999**, *38*, 586) leads to a simple expression for the barrier (eq 29) as an interplay of an intrinsic term and the reaction driving force. The equation predicts barrier heights that are compatible with the BOVB computed barrier heights. Its comparison with the Marcus equation shows similarities and differences.

The field of hydrogen abstraction has traditionally been an area of intense theoretical research. On one hand, the contemporary theoretical tools could all along tackle hydrogen abstraction, because of its relative simplicity. On the other hand, the process is fundamentally important since it is associated with processes that affect "life", such as DNA-damaging, destruction of cell membranes, aging, Alzheimer's disease, oxidation of organic molecules by metallo-enzymes, and so on.[1] As such, there is a great deal of activity, aimed at understanding the reactivity patterns of these reactions and their analogues.[2] Important correlations were established with fundamental factors, such as bond energy, steric effects, the "polar effect", Pauli repulsions, and so on.[2−12] There are not only successes[2a] but also disagreements between different models,[4,5,10a,11b,12] and the goal yet lies ahead. There is still a need for *quantum chemical models* that, on one hand, involve a clear mechanism of barrier formation and, on the other hand, lead to compact expressions of the barrier and its dependence on fundamental properties of the reactant, in a manner that can reveal trends and make systematic predictions, much as the Marcus equation has achieved in the area of electron-transfer reactivity.[13]

A general strategy for modeling can rely either on empirical parameters or on theoretically computed parameters. The inconvenience of empirical modeling, which results in some inconsistency, is that some of the reactivity factors cannot be evaluated from empirical data, and one needs to make assumptions about the missing factors (e.g., the assumption of negligible electronic interaction in electron-transfer transition states[13b]) or estimate them in some independent manner. Pure theoretical modeling is, in this sense, more consistent since all the reactivity factors are available, in principle, from theory. However, the theory-only approach encounters difficulties as well. One of the difficulties in constructing such theoretical models is that computational chemistry methods routinely overestimate barriers, even when sophisticated levels and extended basis sets are used.[14] Fortunately, however, the ab initio barriers calculated for series of hydrogen abstraction reactions often exhibit the same trend as experimental activation energies.[15] Therefore, assuming the correctness of the trends, a consistent and practical approach would be to construct a unified model that reproduces the computed barriers from computed reactivity factors, within the same theoretical methodology.

The choice of theoretical methodology depends, in turn, on a balance of accuracy and insight. MO-based computational methods can be carried out to reasonable accuracies but do not provide direct insight into the factors controlling the barriers. In contrast, valence bond (VB) calculations possess this facility, since the VB barrier can be computed and, using the same computational tools, it can be analyzed in terms of fundamental quantities that are natural concepts of the VB theory, e.g., resonance energies, bond energies, excitation energies, mixing of ionic structures, etc.[16,17] Fortunately, current VB methods, e.g., the breathing orbital VB (BOVB),[18] VBCI,[19] and other VB calculations,[20,21] exhibit a modest accuracy that, for bond energies and barriers, approaches those of MP2 and coupled-cluster CCSD(T) methods. As such, modern VB theory possesses a reasonable mix of the ingredients: accuracy, which is still modest, and great chemical lucidity, that together may enable to construct successful models of reactivity. This is the chosen approach in the present paper, which addresses the barriers of nonidentity hydrogen transfer reactions.

As part of a long-term program to construct VB models of reactivity based on modern VB methods, we have undertaken the approach to use BOVB to calculate barriers, and then to model their heights using VB state correlation diagrams (VBSCD), of the types used before for a variety of reactions.[16,22] In this approach the goal is to construct a general equation that has the following features: (i) it should lead to a physically reasonable mechanism of barrier formation, and (ii) it can reproduce the computed trends and barriers using fundamental

* Corresponding authors.
[†] Xiamen University.
[‡] Université de Paris-Sud.
[§] The Hebrew University.

10.1021/jp026438y CCC: $22.00 
Published on Web 10/24/2002

quantities, e.g., bond energies, resonance energies, excitation energies, etc. We believe that in this manner it would be possible to formulate a correct form of structure−reactivity relationships. Once such goal is achieved, sufficient insight will be gained on the sources of error vis-à-vis experimental barriers in a manner that can be put to practical use.

In a recent paper,[17a] we applied this approach to the barriers of identity reactions, where the hydrogen is transferred between two identical groups, X = X′, in eq 1.

$$X'\bullet + H{-}X \rightarrow X'{-}H + X\bullet \qquad (1)$$

We showed that, for the series, X = X′ = $CH_3$, $SiH_3$, $GeH_3$, $SnH_3$, and $PbH_3$, all computational levels, including MP2, CCSD(T), and BOVB gave the same trend, namely, that the barriers decrease down the column of the periodic table. Using the VBSCD modeling, it was demonstrated that this trend is dominated by a single quantity, the singlet-to-triplet excitation, $\Delta E_{ST}$, of the H−X bond, which is the promotion gap in the VBSCD. Simple equations for the barrier were derived and enabled to predict the trend in the computational barriers for a variety of other X groups. The polar effects,[23] due to the mixing of ionic structures in the transition state, were found[17a] to be significant, but since they behaved as quasi-constants for the entire series, they were not expressed explicitly.

Modeling identity barriers is much easier than nonidentity reaction in which X ≠ X′ in eq 1. One reason is the symmetry of the identity transition state, which makes the VB calculation of the species easy and facilitates the VB expression of all the barrier factors. The other reason is the simplicity of the equation for the barrier that does not include the effect of the reaction energy change (the "driving force" of the reaction). In nonidentity reactions the challenge is much greater, and this is dealt with in the present paper, which seeks to establish a general equation for the barrier that includes dependence on intrinsic factors and the "driving force" of the reaction. In addition, the so-derived barrier equation will have to show the relationship between the barrier of the nonidentity reaction and its constituent identity process and to address the role of the ionic structures whose importance are currently debated in the experimental community.

## Theoretical Methods

**VB Procedures.** In VB theory, a state wave function, Ψ, is given as a linear combination of VB structures, $\Phi_i$, in eq 2.

$$\Psi = \sum_i c_i \Phi_i \qquad (2)$$

The VB structures correspond to all the modes of distributing the "active electrons" that participate in the interchanging bonds. In the case of hydrogen transfer there are three electrons to distribute in the orbitals that define the interchanging bonds along the X−H−X′ axis. These are the active electrons and orbitals that are treated in a VB manner. The rest of the occupied orbitals (the inactive part) are treated as electron pairs in doubly occupied orbitals.

In the BOVB method,[18] the orbitals are allowed to be different for each VB structure. In this manner, the orbitals respond to the instantaneous field of the individual VB structure rather than to an average field of all the structures. As such, BOVB accounts for part of the dynamic correlation, while leaving the wave function compact. For the sake of economy, all the valence orbitals in the present work were allowed to optimize during the BOVB procedure, except for the $\pi$ type orbitals, which were kept frozen.

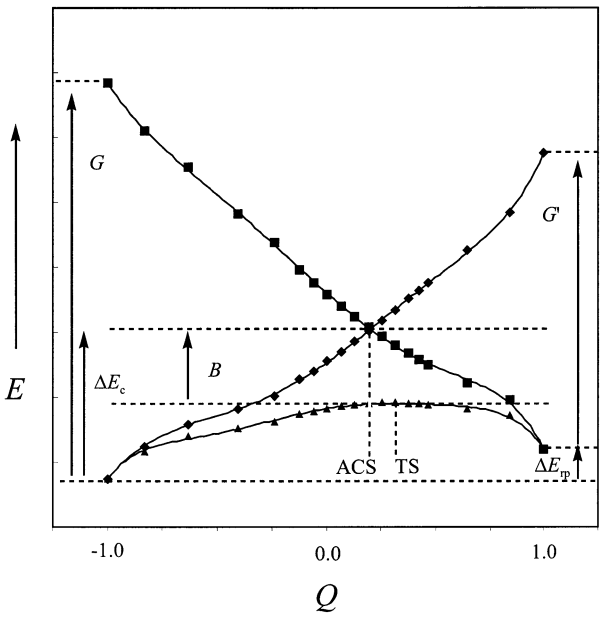


**Figure 1.** A typical VBSCD for X′• + H−X → X′−H + •X, exemplified for X = C and X′ = Si. The locations of the TS and the ACS are indicated along the reaction coordinate *Q* (all points refer to the geometries along the IRC). The *G*s are promotion gaps, the $\Delta E_c$ is the height of the crossing point relative to the reactants, *B* is the resonance energy of the ACS, and $\Delta E_{rp}$ is the reaction energy change.

The weights of the VB structures were determined by use of the Coulson−Chirgwin[24] formula, eq 3, which is the equivalent of a Mulliken population analysis in VB theory.

$$w_i = c_i^2 + \sum_{i \neq j} c_i c_j \langle \Phi_i | \Phi_j \rangle \qquad (3)$$

The calculations used the 6-31G* basis set for X = $CH_3$, $SiH_3$, while for the heavier analogues we used the Los Alamos effective core potential and matching basis set, LANL2DZ, to which we added d-polarization functions taken from 6-31G* (henceforth ECP/31G*).[25] These two basis sets were used before and their compatibility was ascertained. The transition states (TSs) were optimized at the MP2 level and the IRC path[26] was used then as the "reaction coordinate" for the BOVB calculations. Along the IRC path we located also the avoided-crossing state (ACS),[27] which is the state that arises by the mixing of the two Lewis structures at their crossing point. Since the ACS was ascertained to give close barriers to the VB barriers at the MP2 TS (see later), it therefore serves as a model for the TS of the nonidentity reaction.

The reaction coordinate *Q* is defined as the bond order difference:

$$Q = n_1(d') - n_2(d),\ n(d) = e^{-a(d-d_0)} \qquad (4)$$

where $n(d)$ or $n(d')$ are calculated from any given bond length $d$ or $d'$ relative to the equilibrium bond length $d_0$ of X−H (X′−H). The constant $a$ in $n(d)$ is taken from the corresponding values determined before for the identity reaction, where the bond order was defined as 0.5.[17a] With this definition of *Q*, the IRC path stretches from −1 to +1, as shown in Figure 1. The IRC calculations provide the relationship between the bond distances $d'$ (of H−X′) and $d$ (of H−X). Combination of the $d$-$d'$ relationship derived from the IRC with their relationship in eq 4 enables us to determine the individual $d'$ and $d$ lengths for a given value of *Q*. For example, we can determine the $d$-$d'$

**SCHEME 1: VB Structure Set for Hydrogen Transfer Processes (note that the two Lewis structures ($\Phi_L$) are made from covalent and ionic structures)**

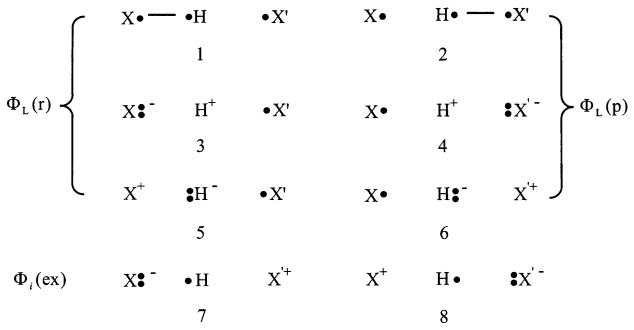


values at $Q = 0$ and compare the location of the ACS relative to the origins of this coordinate (see Appendix 1).

The BOVB calculations were done with the Xiamen package of programs.[28] The MP2 calculations were carried out using Gaussian 98.[29]

**The VB Structures Set.** The VB structures for a hydrogen transfer reaction are shown in Scheme 1 and involve all the modes of distributing three electrons among the three fragments. These are the familiar Heitler−London (HL) structures[30] that describe the covalent spin-pairing in either the right-hand or left-hand bond of the reactants (r) and products (p), respectively, and the corresponding ionic structures, $\Phi_i$, which contribute to the bonds of the reactants and products (r, p) or which are excited states (ex) that can mix only into the TS but not into the ground states of reactants and products.

**VB State Correlation Diagrams (VBSCDs) from the VB Structures.** To convert the VB structures into a compact VBSCD,[16b,17a] the covalent HL structures have to be mixed with the corresponding ionic structures that are required to describe a two-electron Lewis bond. Thus, mixing of $\Phi_{HL}(r)$ with $\Phi_i(r)$, structures **3** and **5**, leads to the right-hand side H−X′ Lewis bond for the reactant X′• /H−X. Similarly, mixing of $\Phi_{HL}(p)$ with $\Phi_i(p)$, structures **4** and **6**, leads to the Lewis bond of the product, X′−H/ •X. Subsequently, the two Lewis curves are computed by tracing them along the IRC that is determined from the MP2 calculations. The crossing point of the two Lewis structures is the location of the ACS, as shown in Figure 1. The wave function of the ACS after avoided crossing is given by the symmetric linear combination of the two Lewis curves, called also the Lewis state, defined in eq 5:

$$\Psi_{L(ACS)} = N[\Phi_L(r) - \Phi_L(p)] \quad N\text{-normalization const.} \quad (5)$$

The full adiabatic state that correspond to the ACS geometry is generated by mixing into $\Psi_L$ the remaining structures, $\Phi_i(ex)$, **7** and **8**:

$$\Psi_{ACS} = c_L\Psi_{L(ACS)} + c_7\Phi_7(ex) + c_8\Phi_8(ex) \quad (6)$$

The individual components of the Lewis state are not frozen and are allowed to relax during the calculations, so that the final adiabatic ACS is the variational mixture of all the eight structures in the VB structure set.

It is apparent that the ACS has a well-defined wave function, which is a perfectly resonating mixture of the principal VB structures, and a well-defined location in the potential energy surface. As such, the ACS is an attractive model for the TS. As shown in Figure 1, however, the ACS is not necessarily identical with the TS. Therefore, before it can be chosen as a model for the TS, one has to show that the ACS is a sufficiently good approximation to the TS.

**TABLE 1: Computed (kcal/mol) Barriers ($\Delta E^{\ddagger}$) and Reaction Energies ($\Delta E_{rp}$) for the Nonidentity Reaction, X′• + H−X → X′−H + •X**

| X,X′ | $\Delta E^{\ddagger}$(MP2) | $\Delta E^{\ddagger}$(VB,TS) | $\Delta E^{\ddagger}$(VB,ACS) | $\Delta E_{rp}$(MP2) | $\Delta E_{rp}$(VB) |
|---|---|---|---|---|---|
| C,Si | 32.4 | 30.7 | 30.5 | 19.7 | 14.6 |
| C,Ge | 34.6 | 33.4 | 32.7 | 26.3 | 21.9 |
| C,Sn | 44.1 | 39.5 | 38.3 | 35.6 | 29.6 |
| C,Pb | 48.3 | 43.0 | 41.2 | 42.3 | 36.0 |
| Si,Ge | 17.1 | 22.3 | 21.9 | 6.6 | 7.3 |
| Si,Sn | 24.9 | 27.0 | 26.0 | 15.9 | 15.0 |
| Si,Pb | 28.5 | 29.9 | 28.1 | 22.6 | 21.4 |
| Ge,Sn | 16.4 | 20.7 | 20.5 | 9.3 | 7.8 |
| Ge,Pb | 19.6 | 22.9 | 22.0 | 16.0 | 14.2 |
| Sn,Pb | 15.1 | 18.2 | 17.9 | 6.7 | 6.4 |

The resonance energy of the ACS is defined in eq 7 and, provided the ACS and TS are close in energy. This would also be the resonance energy of the TS.

$$B = E(\Psi_{ACS}) - E(\Phi_{L,cross}) \sim E(\Psi_{TS}) - E(\Phi_{L,cross}) \quad (7)$$

A related quantity is $B_L$, which is the resonance energy if the ACS is approximated only by the Lewis state (eq 5), namely, the resonance energy of the Lewis state, eq 8:

$$B_L = E(\Psi_{L(ACS)}) - E(\Phi_{L,cross}) \quad (8)$$

The difference $B - B_L$ will account for the importance of the mixing of the excited ionic structures (**7** and **8**), which were found to be of minor importance for the identity reactions.

Another important state function is the linear combination of the HL structures, which cross along the IRC and thereby generate the backbone of the state crossing in the VBSCD. The bonding combination of the HL structures at the crossing point is called the HL-state, given by eq 9, where the *c*'s are coefficients that may or may not be equal (unlike the coefficients of the Lewis structures which are strictly equal at the ACS):

$$\Psi_{HL} = c_r\Phi_{HL}(r) - c_p\Phi_{HL}(p) \quad (9)$$

Thus, while $\Psi_{HL}$ accounts for the covalent three-electron delocalization over the three reaction centers, $\Psi_L$ simply adds the contribution of the ionic fluctuations into the two-electron bonds. The mixing of **7** and **8** further adds to the ACS the charge-transfer fluctuations from one two-electron bond to the other. The energetic effect imparted by mixing of the ionic structure is given by the resonance energy due to covalent−ionic mixing in eq 10.[17a]

$$RE_{cov-ion} = E(\Psi_{ACS}) - E(\Psi_{HL}) \quad (10)$$

This quantity is therefore a direct measure of the "polar effect" in the TS.

## Results

Table 1 shows the energy barriers calculated for all the nonidentity pairs (X,X′) at three different levels: $\Delta E^{\ddagger}$(MP2) data refer to the MP2 barriers, $\Delta E^{\ddagger}$(VB,TS) to the VB barrier calculated at the geometry of the MP2 TS, while $\Delta E^{\ddagger}$(VB,-ACS) data are the barriers calculated at the ACS geometry, with the full wave function in eq 6. Shown also are the reaction energy changes, $\Delta E_{rp}$, for all the pairs. The X, X′ pairs are defined so that the H−X′ bond is always the weaker one.

The deviations between the $\Delta E_{rp}$ quantities at the VB and MP2 level reflect deviations in the corresponding bond energies.[17a]

**TABLE 2: Geometric Features of the TS and ACS for the Nonidentity Reaction, X′• + H−X → X′−H + •X**

| | geometric parameters[a] | | | | | | % deviation[b] (ACS viz TS) | | % extension[c] (ACS) | |
|---|---|---|---|---|---|---|---|---|---|---|
| | TS | | | ACS | | | | | | |
| X,X′ | $d$ (Å) | $d'$ (Å) | $d+d'$ (Å) | $d$ (Å) | $d'$ (Å) | $d+d'$ (Å) | $\%D(d)$ | $\%D(d')$ | $\%\Delta d/d_0$ | $\%\Delta d'/d_0'$ |
| C,Si | 1.536 | 1.637 | 3.173 | 1.444 | 1.721 | 3.165 | −6.0 | 5.1 | 33.8 | 16.0 |
| C,Ge | 1.603 | 1.673 | 3.276 | 1.478 | 1.786 | 3.264 | −7.8 | 6.8 | 37.0 | 15.5 |
| C,Sn | 1.705 | 1.821 | 3.526 | 1.554 | 1.956 | 3.510 | −8.9 | 7.4 | 44.0 | 13.8 |
| C,Pb | 1.779 | 1.821 | 3.600 | 1.600 | 1.977 | 3.577 | −10.0 | 8.6 | 48.3 | 13.6 |
| Si,Ge | 1.857 | 1.763 | 3.620 | 1.804 | 1.815 | 3.619 | −2.9 | 2.9 | 21.6 | 17.4 |
| Si,Sn | 2.010 | 1.868 | 3.878 | 1.899 | 1.974 | 3.873 | −5.5 | 5.7 | 28.1 | 14.8 |
| Si,Pb | 2.134 | 1.843 | 3.977 | 1.968 | 1.999 | 3.967 | −7.8 | 8.5 | 32.7 | 14.8 |
| Ge,Sn | 1.977 | 1.911 | 3.888 | 1.909 | 1.978 | 3.887 | −3.3 | 3.5 | 23.5 | 15.1 |
| Ge,Pb | 2.100 | 1.871 | 3.971 | 1.971 | 1.997 | 3.968 | −6.1 | 6.7 | 27.5 | 14.7 |
| Sn,Pb | 2.123 | 1.940 | 4.063 | 2.061 | 2.007 | 4.068 | −2.9 | 3.5 | 19.9 | 15.3 |

[a] $d$ and $d'$ refer to the drawing in Scheme 2. [b] $\%D(d) = 100[d(\mathrm{ACS}) - d(\mathrm{TS})]/d(\mathrm{TS})$. [c] $\%\Delta d/d_0 = 100[d(\mathrm{ACS}) - d_0]/d_0$.

**SCHEME 2: Definitions of Bond Lengths in the TS and ACS for X′• + H−X → X′−H + •X (X = MH′$_3$, X′ = M′H$_3$)**

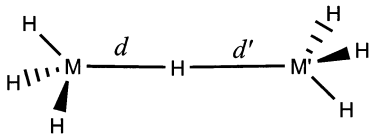


The match between $\Delta E^{\ddagger}$(MP2) and $\Delta E^{\ddagger}$(VB,TS) is not uniform, and the deviations spread from 1.2 kcal/mol for the C, Ge pair to 5.3 kcal/mol for the C, Pb pair. However, what is important in terms of our goal in the present paper is the good match between the $\Delta E^{\ddagger}$(VB,TS) and $\Delta E^{\ddagger}$(VB,ACS) values, which differ by 0.2 to 1.8 kcal/mol. Clearly, therefore, in terms of relative energies, the ACS is a reasonably good approximation to the TS.

Table 2 shows the key geometric features of the TS and the ACS, by reference to the drawing in Scheme 2. The X−H and H−X′ bond lengths of the TS are seen to be different than those of the ACS, by 2.9−10.0% (see $\%D(d,d')$ values). While these deviations are not negligible, it can be seen that the sum of the distances remains nearly constant. This means that the ACS lies on the reaction coordinate and is displaced relative to the TS in a "Hammond fashion",[31] such that one bond gets shorter by the same amount as the second bond gets longer. As shown previously,[27] this is a general phenomenon, and one can locate the ACS by starting at the TS and stepping gradually along the reaction vector, which is the mode having an imaginary frequency in the TS. The displacement is therefore linear, and as such the ACS and the TS are located within the avoided crossing region. As discussed quite sometime ago,[32] the resonance energy $B$ remains constant along such a displacement. We may therefore use the ACS as an approximation to the TS by the following equation:

$$\Psi_{\mathrm{TS}} \approx \Psi_{\mathrm{ACS}} = c_{\mathrm{L}}\Psi_{\mathrm{L(ACS)}} + c_7\Psi_7(\mathrm{ex}) + c_8\Psi_8(\mathrm{ex}) \quad (11)$$

and use the ACS henceforth for the purpose of modeling the barrier.

Table 3 lists a few properties of the ACS for the X′, X pairs. The first three lines show the weights of the covalent, ionic, and excited-ionic structures (depicted in Scheme 1). The ACS species are primarily covalent, but all have significant ionic contributions which amount to as much as 31−37% of the total weight. The ionicity of the ACS is more significant than in the ground states where the weights of the ionic structures reach 21−28%. The TS ionicity is accompanied by large covalent-ionic resonance energy, in the fourth line of the Table. This quantity, $RE_{\mathrm{cov-ion}}$, is seen to be almost a constant, ca. 20 kcal/mol, and does not vary in relation to the weight of the ionic structures. The excited-ionic structures are seen to have much smaller weights compared with the other ionic structures. Their energetic effect is given by the difference of the $B$ and $B_{\mathrm{L}}$ quantities, which is seen to be small, ca. 3.9−5.5 kcal/mol, and almost constant. Thus, much like in the study of the identity reactions,[17a] here too the TS is dominated by the avoided crossing of the Lewis curves. The polar effect in the TS is significant but it continues to behave as a quasi-constant quantity.

The resonance energy of the TS, $B$, exhibits intriguing equalities, e.g., $B$(C,Ge) = $B$(Si,Ge), $B$(C,Pb) = $B$(Si,Pb) = $B$(Ge,Pb) = $B$(Sn,Pb), etc. Moreover, $B$(X,X′) for the nonidentity reaction has virtually the same value as $B$(X′,X′) in the identity reactions[17a] and has no relationship to $B$(X,X). It seems that the resonance energy of the TS is determined by the weak bond, H−X′. In fact, $B$ can be reasonably well approximated as follows:

$$B \approx 0.5D(\mathrm{H-X'})_0 \quad (12)$$

where the subscript zero refers to the bond at its equilibrium geometry. This expression is reminiscent of the similar expression derived for the resonance energy of the identity TS.[17a] However, the relation to the weak bond only is intriguing and will have to be accounted for in terms of the mechanism of avoided crossing.

## Discussion

**The Mechanism of Activation.** As shown in Figure 1, the ACS is achieved by the crossing of the two Lewis curves, where the two Lewis structures balance their energies. This is expressed in eq 13:

$$E(\Phi_{\mathrm{L}}(r), \mathrm{X'\bullet\ H-X})^{\ddagger} = E(\Phi_{\mathrm{L}}(\mathrm{p}), \mathrm{X'-H\ \bullet X})^{\ddagger} \quad (13)$$

where the double dagger refers to the structures at their ACS geometry. The condition for achieving this energy equality can be derived using the expressions of the semiempirical VB,[33,34] discussed in previous publications[17a] (see Appendix in ref 17a). Thus, the energy of the bond is given by $-\lambda$, while the nonbonded repulsion is given by $\lambda_{\mathrm{T}}$, where the subscript, T, refers to the triplet Pauli repulsion.[17a,33] Using these two

**TABLE 3: BOVB Calculated Quantities for the ACS: Weights ($\omega$) of Covalent and Ionic Structures, Covalent−Ionic Resonance Energies ($RE_{cov-ion}$), and ACS Resonance Energies ($B$ and $B_L$)**

| | C,Si | C,Ge | C,Sn | C,Pb | Si,Ge | Si,Sn | Si,Pb | Ge,Sn | Ge,Pb | Sn,Pb |
|---|---|---|---|---|---|---|---|---|---|---|
| $\omega_{cov}$ | 0.631 | 0.655 | 0.682 | 0.689 | 0.608 | 0.619 | 0.632 | 0.640 | 0.651 | 0.634 |
| $\omega_i$(r,p) | 0.312 | 0.303 | 0.272 | 0.265 | 0.331 | 0.319 | 0.304 | 0.305 | 0.289 | 0.306 |
| $\omega_i$(ex) | 0.057 | 0.042 | 0.046 | 0.046 | 0.061 | 0.062 | 0.064 | 0.055 | 0.060 | 0.060 |
| $RE_{cov-ion}$[a] | 24.9 | 24.8 | 21.3 | 20.5 | 22.7 | 20.3 | 19.6 | 20.7 | 19.9 | 19.7 |
| $B_L$ (kcal/mol)[b] | 34.7 | 33.4 | 29.0 | 27.1 | 34.2 | 30.2 | 27.6 | 30.4 | 28.0 | 27.8 |
| $B$ (kcal/mol)[c] | 40.0 | 38.9 | 33.7 | 31.4 | 38.8 | 34.2 | 31.5 | 35.0 | 32.4 | 31.9 |

[a] See eq 10. [b] See eq 8. [c] See eq 7.

**TABLE 4: Semiempirical Energies of the Lewis Structures, X′• H−X and X′−H •X, at the ACS (kcal/mol)[a]**

| | C,Si | | C,Ge | | C,Sn | | C,Pb | | Si,Ge | | Si,Sn | | Si,Pb | | Ge,Sn | | Ge,Pb | | Sn,Pb | |
|---|---|---|---|---|---|---|---|---|---|---|---|---|---|---|---|---|---|---|---|---|
| | C | Si | C | Ge | C | Sn | C | Pb | Si | Ge | Si | Sn | Si | Pb | Ge | Sn | Ge | Pb | Sn | Pb |
| $\lambda$ | 72.0 | 67.7 | 68.5 | 63.2 | 61.3 | 57.7 | 57.4 | 54.8 | 62.7 | 61.9 | 57.1 | 56.9 | 53.1 | 53.8 | 55.8 | 56.7 | 52.4 | 53.9 | 52.7 | 53.4 |
| $\lambda_T$ | 85.4 | 102.8 | 79.1 | 94.7 | 67.0 | 83.1 | 60.6 | 72.0 | 89.1 | 91.6 | 75.7 | 80.7 | 66.7 | 69.7 | 76.6 | 80.3 | 68.7 | 69.9 | 69.6 | 68.8 |
| $\lambda+0.5\lambda_T$ | 114.7 | 119.2 | 108.1 | 110.6 | 94.8 | 99.3 | 87.7 | 90.8 | 107.2 | 107.7 | 95.0 | 97.2 | 86.4 | 88.7 | 94.1 | 96.9 | 86.7 | 88.8 | 87.5 | 87.8 |

[a] Based on eq 15.

definitions, the energies of the two Lewis structures are expressed in eqs 14a and 14b,

$$E(\Phi_L(r), X'\bullet H{-}X)^{\ddagger} = -\lambda(H{-}X)^{\ddagger} + 0.5[\lambda_T(X',H) + \lambda_T(X,X')]^{\ddagger} \quad (14a)$$

$$E(\Phi_L(p), X'{-}H \bullet X)^{\ddagger} = -\lambda(H{-}X')^{\ddagger} + 0.5[\lambda_T(X,H) + \lambda_T(X,X')]^{\ddagger} \quad (14b)$$

where $\lambda_T(X,X')^{\ddagger}$ refers to the triplet repulsion[11] of the end groups, X and X′, in the ACS. Thus, in each Lewis structure, there are triplet repulsions between the α spin electron of the nonbonded group, X (or X′), and the electrons of the H−X′(X) bond, which have 50% distribution of spins α and $\beta$.[33b] This equation neglects steric effect of these groups and electrostatic interactions between the nonbonded X (X′) group and H. The condition for crossing becomes then

$$\lambda(H{-}X')^{\ddagger} + 0.5\lambda_T(X',H)^{\ddagger} = \lambda(H{-}X)^{\ddagger} + 0.5\lambda_T(X,H)^{\ddagger} \quad (15)$$

Table 4 shows the semiempirical quantities evaluated from the BOVB data for all the ACS structures of this study, denoted by the X, X′ pairs. It can be seen that in most cases the condition of eq 15 is met precisely, while in some cases there are discrepancies of 2.2−4.5 kcal/mol, which may reflect the neglect of the electrostatic and steric interactions in eqs 14a and 14b.

Assuming that $\lambda_T$ is proportional to $\lambda$ by roughly a constant, then the condition in eq 15 becomes simply eq 16. Such a condition has traditionally been used in other approaches that employ empirical bond energy curves to obtain the crossing point.[2a,11]

$$\lambda(H{-}X')^{\ddagger} \approx \lambda(H{-}X)^{\ddagger} \quad (16)$$

The data in Table 4 show that this condition is approximately met in the various ACS structures. This means that in the ACS, the stronger bond will have to be weakened much more than the weak bond to attain the crossing and the above equality. Indeed, inspection of Table 2 shows that in each case, the weak bond, H−X′, undergoes a smaller percentage of lengthening ($\%\Delta d'/d_0' = 13.6{-}17.4$) compared with the strong bond, X−H ($\%\Delta d/d_0 = 19.9{-}48.3$). At the asymptote, we might consider that the weak bond retains its original strength and only the strong bond stretches to achieve bond strength equality with the weak bond. Thus, we should expect that the properties of the TS (ACS) will be determined much by the weak bond.

**TABLE 5: Comparison of Semiempirical and BOVB Calculated Resonance Energies for the ACS (kcal/mol)**

| X,X′ | $B$(VB) | $B_L$(VB) | $B$(eq 18) | $B$(eq 12) |
|---|---|---|---|---|
| C,Si | 40.0 | 34.7 | 39.0 | 42.1 |
| C,Ge | 38.9 | 33.4 | 36.4 | 38.8 |
| C,Sn | 33.7 | 29.0 | 32.4 | 34.2 |
| C,Pb | 31.4 | 27.1 | 29.7 | 30.8 |
| Si,Ge | 38.8 | 34.2 | 35.8 | 38.8 |
| Si,Sn | 34.2 | 30.2 | 32.0 | 34.2 |
| Si,Pb | 31.5 | 27.6 | 29.2 | 30.8 |
| Ge,Sn | 35.0 | 30.4 | 31.8 | 34.2 |
| Ge,Pb | 32.4 | 28.0 | 29.3 | 30.8 |
| Sn,Pb | 31.9 | 27.8 | 29.2 | 30.8 |

**The Resonance Energy of the ACS.** Using the same semiempirical VB theory,[33] we can derive an expression for $B$, using the mixing of the two VB structures. The details are given in Appendix 2 to this paper, while eq 17 shows the result:

$$B = \frac{1}{3}[\lambda(H{-}X) + 0.5\lambda_T(H,X) - 0.5\lambda_T(X,X') - \lambda(X,X')]^{\ddagger} \quad (17)$$

An identical expression exists by replacing the $[\lambda(H{-}X) + 0.5\lambda_T((H,X)]^{\ddagger}$ term by the $[\lambda(H{-}X) + 0.5\lambda_T(H,X')]^{\ddagger}$ term, since they are equal according to eq 15. Neglecting the long-range terms, the expression for $B$ becomes

$$B = \frac{1}{3}[\lambda(H{-}X') + 0.5\lambda_T(H,X')]^{\ddagger} = \frac{1}{3}[\lambda(H{-}X) + 0.5\lambda_T(H,X)]^{\ddagger} \quad (18)$$

Because the primed and unprimed $[\lambda + \lambda_T]^{\ddagger}$ values are a bit different (see Table 4), we take an average value for $B$. These $B$ values are presented in Table 5, along with the VB calculated quantities and those estimated from eq 12 above. The match of the calculated values to the estimated values is reasonably good. The $B$(eq 18) values are lower somewhat than the $B$(VB) values, by 2.1 ± 1 kcal/mol. The $B$(eq 12) values are closer to the $B$(VB) values. Because eq 12 is much simpler, it should be the choice expression whenever eq 18 cannot be applied.

It should be noted, that the singlet−triplet excitation energy of the bond (H−X or H−X′) is given by the sum $[\lambda + \lambda_T]$.

**TABLE 6: Comparison of Heights of the Crossing Points (in kcal/mol) for the Nonidentity Reaction, X′• + H−X → X′−H + •X, Computed by BOVB and a Semiempirical Model Equation (eq 22)**

| | C,Si | C,Ge | C,Sn | C,Pb | Si,Ge | Si,Sn | Si,Pb | Ge,Sn | Ge,Pb | Sn,Pb |
|---|---|---|---|---|---|---|---|---|---|---|
| $\Delta E_c$(VB) | 70.5 | 71.6 | 72.0 | 72.6 | 60.7 | 60.2 | 59.6 | 55.5 | 54.3 | 49.8 |
| $\Delta E_c$(eq 22) | 74.4 | 72.0 | 74.5 | 73.3 | 57.1 | 59.7 | 58.8 | 54.3 | 52.8 | 46.1 |

Thus, assuming that $\lambda \approx \lambda_T$, then the expression in eq 19 is identical to the expression derived for the identity reactions,[17a] namely,

$$B = 0.25\Delta E_{ST}(\mathrm{H{-}X})^{\ddagger} = 0.25\Delta E_{ST}(\mathrm{H{-}X'})^{\ddagger} \quad (19)$$

where all these terms correspond to their values at the ACS geometry, indicated by the double dagger. The success of eq 12 is surprisingly good and indicates that at the ACS geometry the originally weak bond H−X′ stretches to an extent that its singlet−triplet excitation energy, $\Delta E_{ST}(\mathrm{H{-}X'})^{\ddagger}$, is related to the original bond energy, $D(\mathrm{H{-}X'})_0$, as follows:

$$\Delta E_{ST}(\mathrm{H{-}X'})^{\ddagger} = 2D(\mathrm{H{-}X'})_0 \Rightarrow B = 0.5D(\mathrm{H{-}X'})_0 \quad (20)$$

**Expressions for the Barrier.** Using Figure 1, the barrier in any direction is given by the difference between the height of the corresponding crossing point and the resonance energy, i.e.,

$$\Delta E^{\ddagger} = \Delta E_c - B \quad (21)$$

This expression enables us to estimate the barrier and relate it to the BOVB computed one, given by the difference $E$(ACS) − $E(\mathrm{X'\bullet} + \mathrm{H{-}X})_0$, where the subscript zero refers to the reactants. Two complementary approaches are used henceforth to derive barriers based on the mechanism of activation projected by the VBSCD.

The first approach relies on the semiempirical expression in eq 14. Thus, the height of the crossing point is given by the energy difference of the Lewis structure at the ACS and at the ground state. Using the Lewis structure with the weak bond H−X′, this becomes

$$\Delta E_c = \lambda'_0 - \lambda(\mathrm{H{-}X'})^{\ddagger} + 0.5[\lambda_T(\mathrm{X,H}) + \lambda_T(\mathrm{X,X'})]^{\ddagger} \quad (22)$$

Here the $\lambda'_0 - \lambda(\mathrm{H{-}X'})^{\ddagger}$ term corresponds to the bond distortion energy required to reach the ACS from the ground state, while the other two terms correspond to the triplet repulsion that occurs by bringing the nonbonded X to the H−X′ molecule.[17a,33] The so-determined values are shown in Table 6 side by side with the heights of the crossing point obtained from the BOVB calculations. The match is seen to be very reasonable, considering the fact that eq 22 neglects other nonbonded interactions. Clearly, eq 22 can be further refined by accounting for the nonbonded interactions. A similar semiempirical approach is described in ref 11a−c and leads to a very good fit to experimental barriers. However, as we elaborated before,[33b] this model keeps the small long-range repulsion term, $\lambda_T$(X,X′), and neglects the large short-range repulsion terms, e.g., $\lambda_T$(X,H). We interpreted the success of this approach as being due to cancellation of errors.[33b]

An alternative and independent approach is to evaluate the height of the avoided crossing from the promotion gaps, curvatures, and other properties of the BOVB curves in Figure 1. For an identity reaction, the height of the crossing point is related to the promotion gap of the VBSCD as follows:[16]

$$\Delta E_c = fG \quad (23)$$

where $f$ is some fraction of the promotion gap, $G$, that separates the two Lewis curves at their onset ($Q = \pm 1$) in Figure 1.

For a nonidentity reaction, as in Figure 1, there are two different gaps $G'$ and $G$. Similarly, there are two different corresponding $f$ factors ($f$ and $f'$) that describe the curvatures of the corresponding curves in Figure 1. In addition, the ground state points of the Lewis curves maintain an energy difference, given as the difference in the corresponding bond energies,

$$\Delta E_{rp} = E(\mathrm{p}) - E(\mathrm{r}) = D(\mathrm{H{-}X})_0 - D(\mathrm{X{-}H'})_0 \quad (24)$$

Combining all these factors into a single equation for the barrier,[16b,22b] derived in Appendix 3 to this paper, and defining average gap and $f$ quantities, as in eqs 25a and 25b

$$G_a = 0.5\,(G + G') \quad (25a)$$

$$f_a = 0.5\,(f + f') \quad (25b)$$

leads to the expression of $\Delta E_c$ in eq 26

$$\Delta E_c = f_a G_a + \left(\frac{G'}{2G_a}\right)\Delta E_{rp} + \left(\frac{1}{2G_a}\right)\Delta E_{rp}^2 \quad (26)$$

Neglecting the quadratic term, and assuming that $G'/2G_a$ is $\sim$1/2, leads to the following compact expression:

$$\Delta E_c = f_a G_a + \frac{1}{2}\Delta E_{rp} \quad (27)$$

The quantities $G$, $G'$, and $\Delta E_{rp}$ are available directly from the VB calculations and are collected in Table 7. The $f$ and $f'$ values are derived from the VB curves at $Q = 0$ (see Appendix 1 and 3). The quantities $G$ and $G'$ are identical to the corresponding quantities in the identity reactions and can be related to the singlet−triplet excitation of the corresponding H−X and H−X′ bonds, that is:

$$G \approx 0.75\Delta E_{ST}(\mathrm{H{-}X});\ G' \approx 0.75\Delta E_{ST}(\mathrm{H{-}X'}) \quad (28)$$

In the identity process, the $f$ factor was almost constant 0.38−0.40 for the entire series. Here, the two factors are different such that the curve along which the stronger bond is made is more concave and has the smaller value.[16b] However, the average quantity $f_a$ is less variable, $f_a = 0.34{-}0.40$, and is closer to the corresponding quantity in the identity reactions. Using all these quantities in eqs 26 and 27 leads to the $\Delta E_c$ values in Table 7. Comparison with the corresponding BOVB values shows a very good fit. Thus, in eq 26, the coefficient of the linear term, $G'/2G_a$, is smaller than 1/2, so that the use of 1/2 in eq 27 compensates for the quadratic term in eq 26.

Equation 27 leads to a compact expression for the energy barrier in eq 29:

$$\Delta E^{\ddagger}(\mathrm{VBSCD}) = f_a G_a + 0.5\Delta E_{rp} - B \quad (29)$$

**TABLE 7: Reactivity Factors and Heights of the Crossing Points Calculated from the VBSCD and by Direct BOVB Computations[a]**

| | C,Si | C,Ge | C,Sn | C,Pb | Si,Ge | Si,Sn | Si,Pb | Ge,Sn | Ge,Pb | Sn,Pb |
|---|---|---|---|---|---|---|---|---|---|---|
| $f$ | 0.34 | 0.30 | 0.30 | 0.30 | 0.37 | 0.34 | 0.32 | 0.36 | 0.33 | 0.37 |
| $f'$ | 0.41 | 0.41 | 0.40 | 0.38 | 0.42 | 0.43 | 0.41 | 0.40 | 0.38 | 0.39 |
| $G$ | 192.9 | 192.9 | 192.9 | 192.9 | 144.3 | 144.3 | 144.3 | 145.7 | 145.7 | 124.2 |
| $G'$ | 144.3 | 145.7 | 124.2 | 115.8 | 145.7 | 124.2 | 115.8 | 124.2 | 115.8 | 115.8 |
| $\Delta E_{rp}$ | 14.6 | 21.9 | 29.6 | 36.0 | 7.3 | 15.0 | 21.4 | 7.8 | 14.2 | 6.4 |
| $\Delta E_c$(eq 26) | 70.1 | 70.9 | 69.8 | 70.2 | 61.1 | 59.5 | 58.8 | 55.1 | 53.5 | 48.9 |
| $\Delta E_c$(eq 27) | 70.5 | 71.1 | 70.3 | 70.5 | 60.9 | 59.2 | 58.2 | 55.2 | 53.5 | 48.8 |
| $\Delta E_c$(VB) | 70.5 | 71.6 | 72.0 | 72.6 | 60.7 | 60.2 | 59.6 | 55.5 | 54.3 | 49.8 |

[a] Except for the dimensionless $f$'s all other factors are in kcal/mol.

**TABLE 8: Comparison of Barriers and Intrinsic Barriers for X′,X Pairs, Calculated Using the VBSCD Model Equation and the Marcus Equation with the Values Computed by BOVB[a]**

| | C,Si | C,Ge | C,Sn | C,Pb | Si,Ge | Si,Sn | Si,Pb | Ge,Sn | Ge,Pb | Sn,Pb |
|---|---|---|---|---|---|---|---|---|---|---|
| $\Delta E^{\ddagger}$(eq 29) | 30.2 | 31.9 | 36.4 | 38.8 | 21.9 | 25.1 | 27.2 | 19.8 | 21.1 | 17.2 |
| $\Delta E^{\ddagger}$(Marcus) | 29.0 | 33.0 | 36.7 | 40.3 | 22.4 | 25.4 | 28.2 | 20.7 | 23.1 | 17.0 |
| $\Delta E^{\ddagger}$(VB,ACS) | 30.5 | 32.7 | 38.3 | 41.2 | 21.9 | 26.0 | 28.1 | 20.5 | 22.0 | 17.9 |
| $\Delta E^{\ddagger}$(VB,TS) | 30.7 | 33.4 | 39.5 | 43.0 | 22.3 | 27.0 | 29.9 | 20.7 | 22.9 | 18.2 |
| $\Delta E_0^{\ddagger}$(Marcus) | 21.1 | 20.6 | 19.1 | 17.7 | 18.6 | 17.1 | 15.7 | 16.6 | 15.2 | 13.7 |
| $\Delta E_{int}^{\ddagger}$(eq 31) | 23.5 | 21.4 | 22.9 | 22.0 | 18.2 | 18.2 | 16.8 | 16.6 | 14.7 | 14.6 |

[a] All values are in kcal/mol.

In this manner, the equation contains a balance between an intrinsic term, $f_a G_a$, and the reaction "driving force" term, $\Delta E_{rp}$. Using the BOVB computed $B$ values we obtain the barriers according to eq 29. These barriers are compared with the BOVB barriers in Table 8 and the fit is seen to be very good. Clearly, eq 29, based on the VBSCD, captures the key factors that determine the barrier, and can form a basis for structure−reactivity relationships.

It is instructive to compare eq 29 with the Marcus expression for the barrier[13] in terms of the intrinsic barrier, $\Delta E_0^{\ddagger}$, and the reaction energy, $\Delta E_{rp}$, as shown in eq 30.

$$\Delta E^{\ddagger}(\text{Marcus}) = \Delta E_0^{\ddagger} + 0.5\Delta E_{rp} + \frac{\Delta E_{rp}^2}{16\Delta E_0^{\ddagger}} \qquad (30)$$

Much like the Marcus equation, the VBSCD eq 29 contains a balance of an intrinsic barrier quantity and the reaction energy term (the correlation coefficient $r^2$ between the two sets of barriers is 0.9851). In the Marcus equation, the intrinsic barrier, $\Delta E_0^{\ddagger}$, is determined as the average of the component identity barriers. In the VBSCD equation, the intrinsic barrier in the VBSCD follows the expression

$$\Delta E_{int}^{\ddagger} = f_a G_a - B \qquad (31)$$

and can be determined as such even when the process has no identity components (e.g., radical addition, etc.). Using eq 31, the VBSCD barrier becomes

$$\Delta E^{\ddagger}(\text{VBSCD}) = \Delta E_{int}^{\ddagger} + 0.5\Delta E_{rp} \qquad (32)$$

Table 8 shows the intrinsic barriers, and the barriers calculated with the Marcus and VBSCD equations, alongside the BOVB calculated barriers for the ACS and the MP2 TS. It is apparent that the intrinsic barriers in the Marcus equation are smaller than the corresponding quantity in the VBSCD equation. This difference is compensated in the Marcus expression by the quadratic term, while in the VBSCD equation this term is unnecessary. Both equations give very good fits to the BOVB barriers determined for the ACS and the MP2 TS. As such, the VBSCD equation can serve as a general organizing tool for structure reactivity relationships.

## Conclusions

The paper presents BOVB computations for nonidentity hydrogen transfer reactions between X and X′ groups, X ≠ X′ = $CH_3$, $SiH_3$, $GeH_3$, $SnH_3$, $PbH_3$. The VBSCD model[16] and a semiempirical VB theory[17a,33] are then used to pattern the computational BOVB results. It is shown that the avoided crossing state (ACS)[27] is a reasonable approximation to the BOVB transition state. The ACS is the state obtained from the avoided crossing of the two Lewis structures of reactants and products and contains additional contributions from excited charge-transfer VB configurations (structures **7** and **8** in Scheme 2). The calculations show that the weaker bond, defined as X′−H, dominates the properties of the ACS; its geometry and resonance energy. However, the barrier itself is affected more by the stretching of the strong bond (throught the $fG$ quantity in eq 27). As found for the corresponding identity reactions,[17a] here too the polar effect in the transition states is significant but behaves as a quasi-constant quantity.

A simple expression derived from the VBSCD model reproduces the BOVB barriers quite well. Thus, it is shown that a qualitative model can be coupled to a complex computational scheme to reproduce all the trends and show their dependence on fundamental properties of the reactant and products. Comparable to the Marcus equation, the VBSCD expression of the barrier contains a balance between intrinsic properties of reactants and the reaction driving force. The intrinsic barrier can be derived from the properties of the reactants and does not require knowledge of the identity barriers as the Marcus equation.

**Acknowledgment.** The research at XMU is supported in part by the Natural Science Foundation of China (No. 20073033, No. 20021002) and by the Ministry of Education, China. The research at HU is supported in parts by the VW Stiftung through the Ministry of Sciences of the Niedersachsen States and by the Robert Szold Foundation.

**TABLE A1: *d* and *d′* values for $Q = 0$ and *Q* values for ACS**

| | C,Si | C,Ge | C,Sn | C,Pb | Si,Ge | Si,Sn | Si,Pb | Ge,Sn | Ge,Pb | Sn,Pb |
|---|---|---|---|---|---|---|---|---|---|---|
| *d* (Å) | 1.354 | 1.365 | 1.397 | 1.424 | 1.779 | 1.813 | 1.859 | 1.851 | 1.891 | 2.030 |
| *d′* (Å) | 1.807 | 1.890 | 2.100 | 2.138 | 1.840 | 2.058 | 2.105 | 2.036 | 2.076 | 2.038 |
| *Q*(ACS) | 0.21 | 0.24 | 0.32 | 0.33 | 0.06 | 0.18 | 0.22 | 0.13 | 0.17 | 0.08 |

## Appendix 1. *d* and *d′* values for $Q = 0$ and *Q* values for ACS Structures

The location of $Q = 0$ is necessary for obtaining the values of *f* and *f′* for the two intersecting VB curves. This is done as follows. (i) Using the IRC calculations we obtain the values of *d′* as a function of *d*. (ii) From eq 4 (text), at $Q = 0$, we have the relationship

$$a(d - d_0) = a'(d' - d_0') \tag{A.1}$$

where *a* and *a′* are the constants which are obtained by setting the bond order in the identity transition state to 0.5.

Table A1 gives the bond lengths for the structures at $Q = 0$. Also shown are the *Q* values of the ACS, which are obtained by use of the *d* and *d′* lengths in Table 2 to determine the bond orders of the ACS and obtain *Q*(ACS) from eq 4.

## Appendix 2. Derivation of Resonance Energy between Two Lewis Structures

To get an expression for resonance energy between the two Lewis structures, a secular equation for the two structures is solved.

From the semiempirical VB theory,[33,34] the energies of the two Lewis structures are given as

$$H_{11} = E(\Phi_L(r), X'\bullet H{-}X) = -\lambda(H{-}X) + 0.5[\lambda_T(X',H) + \lambda_T(X,X')] \tag{A2.1}$$

$$H_{22} = E(\Phi_L(p), X'{-}H\bullet X) = -\lambda(H{-}X') + 0.5[\lambda_T(X,H) + \lambda_T(X,X')] \tag{A2.2}$$

And their interaction is

$$H_{12} = \langle\Phi_L(r)|\mathbf{H}|\Phi_L(p)\rangle = 0.5[\lambda(H{-}X) + \lambda(H{-}X') - \lambda(X{-}X') - \lambda_T(X,X')] \tag{A2.3}$$

$$S_{12} = \langle\Phi_L(r)|\mathbf{H}|\Phi_L(p)\rangle = -0.5 \tag{A2.4}$$

At the ACS geometry, the energies of the two Lewis structures are identical. Thus, the energy $E(\Psi_{L(ACS)})$ is easily given by solving the $2 \times 2$ secular equation

$$E(\Psi_{L(ACS)}) = H_{11} - \frac{H_{12} - S_{12}H_{11}}{1 - S_{12}} \tag{A2.5}$$

From eqs A2.1, A2.2, and A2.4 we have

$$\begin{aligned} B &= E(\Phi_L(r), X'\bullet H{-}X) - E(\Psi_{L(ACS)}) \\ &= \frac{2}{3}(H_{12} + 0.5H_{11}) \\ &= \frac{1}{3}[\lambda(H{-}X) + 0.5\lambda_T(X,H) - \lambda(X{-}X') - 0.5\lambda_T(X,X')] \end{aligned} \tag{A2.6}$$

All parameters on the right-hand side in eq A2.6 are related to the ACS geometry. Thus we get eq 16 in the text.

## Appendix 3. Derivation of Barrier Equation for the Two-Curve VBSCD

Suppose that the energies of the two curves are written as quadratic functions of the reaction coordinate *Q*,[22b]

$$E_r(Q) = a_0 + a_1Q + a_2Q^2 \tag{A3.1}$$

$$E_p(Q) = b_0 + b_1Q + b_2Q^2 \tag{A3.2}$$

The coefficients of $a_i$ and $b_i$ are defined so as to match the idea inherent in the VBSCD (see pp 128−131 in ref 22b) that the height of the crossing point, eq 23, relative to the reactant state can be expressed as a fraction (*f*) of the promotion gap (*G*). Thus, the coefficients are expressed, by reference to Figure A1, as follows:

$$a_0 = f_rG_r^p, a_1 = \frac{1}{2}G_r^p, a_2 = \left(\frac{1}{2} - f_r\right)G_r^p \tag{A3.3}$$

$$b_0 = \Delta E_{rp} + f_pG_p^r, b_1 = -\frac{1}{2}G_p^r, b_2 = \left(\frac{1}{2} - f_p\right)G_p^r \tag{A3.4}$$

With these coefficients the $f_r$ and $f_p$ values are simply the slopes of the VB curves at $Q = 0$ and are obtained as follows:

$$E_r(0) = f_rG_r^p \tag{A3.5}$$

$$E_p(0) = f_pG_p^r + \Delta E_{rp} \tag{A3.6}$$

where

$$G_r^p = G_p + \Delta E_{rp} \tag{A3.7}$$

$$G_p^r = G_r - \Delta E_{rp} \tag{A3.8}$$

Having $E(0)$ and *G* value leads to the *f* values. The so-determined *f* values are the *f* and *f′* in Table 7 in the text. At the crossing point $Q_c$, the energies of the two structures are identical. Neglecting the quadratic terms from eqs A3.1 and A3.2 we have

$$Q_c = \frac{2(f_pG_p^r - f_rG_r^p + \Delta E_{rp})}{G_p^r + G_r^p} \tag{A3.9}$$

Substituting this $Q_c$ value into eq. A3.1 we get[16b,22b]

$$\Delta E_c = \frac{(f_p + f_r)G_p^rG_r^p}{G_p^r + G_r^p} + \frac{G_r^p\Delta E_{rp}}{G_p^r + G_r^p} \tag{A3.10}$$

where the quadratic terms in eq A3.1 are still neglected.

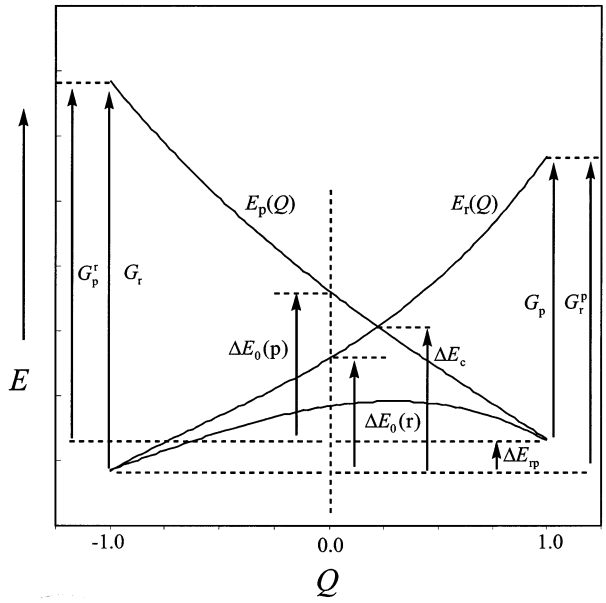


**Figure A1.** VBSCD showing the parameters needed to derive a barrier expression for a nonidentity reaction.

Define the parameter, Δ,

$$\frac{G_p^r - G_r^p}{G_p^r + G_r^p} = \Delta \qquad \text{(A3.11)}$$

If Δ is an infinitesimal, it can be proven that

$$\frac{G_p^r G_r^p}{G_p^r + G_r^p} = \frac{1}{4}(G_p^r + G_r^p) + O(\Delta^2) \qquad \text{(A3.12)}$$

By neglecting the quadratic terms of the infinitesimal, eq A3.10 is written as

$$\Delta E_c = f_a G_a + \frac{G_p}{2G_a}\Delta E_{rp} + \frac{1}{2G_a}\Delta E_{rp}^2 \qquad \text{(A3.13)}$$

where

$$f_a = \frac{1}{2}(f_p + f_r)$$

$$G_a = \frac{1}{2}(G_p^r + G_r^p) = \frac{1}{2}(G_p + G_r) \qquad \text{(A3.14)}$$

In applications, $f_p$ and $f_r$ are given by eqs. A3.5 and A3.6. In the nonidentity hydrogen transfer reaction,

$$G_r = G, \quad G_p = G', \quad f_r = f, \quad f_p = f' \qquad \text{(A3.15)}$$

Thus, we finally get eq 26 in the main text.

## References and Notes


(1) For example, (a) Borman, S. *C&E News* **1994**, April 18, 4. (b) See for example, Giese, B.; Graph, X. B.; Burger, J.; Kesselheim, J.; Senn, M.; Schäfer, T. *Angew. Chem., Int. Ed.* **1993**, *32*, 1742. (c) See for example, Groves, J. T. *J. Chem. Educ.* **1985**, *62*, 928. (d) Halliwell, B.; Gutteridge, J. M. C. *Free Radicals in Biology and Medicine*, 2nd ed.; Clarendon Press: Oxford, 1989. (e) Varadarajan, S.; Kanski, J.; Aksenova, M.; Lauderback, C.; Butterfield, D. A. *J. Am. Chem. Soc.* **2001**, *123*, 5625. (f) Rauk, A.; Armstrong, D. A.; Fairlie, D. P. *J. Am. Chem. Soc.* **2000**, *122*, 9761. (g) Hoffner, J.; Schottelius, M. J.; Feichtinger, D.; Chen, P. *J. Am. Chem. Soc.* **1998**, *120*, 376.

(2) For some reviews on reactivity trends in hydrogen transfer reactions, see: (a) Arnuat, L. G.; Pais, A. A. C. C.; Formosinho, S. J. *J. Mol. Struct. (THEOCHEM)* **2001**, *563/4*, 1. (b) Mayer, J. M. In *Biomimetic Oxidations Catalyzed by Transition Metals*; Meunier, B. M., Ed.; Imperial College Press: London, 1999; Ch 1, pp 1−44. (c) Gardner, K. A.; Mayer, J. M. *Science* **1995**, *269*, 1849. (d) Albu T. V.; Corchodo J. C.; Truhlar D. G. *J. Phys. Chem. A* **2001**, *105*, 8465. (e) Parr, C. A.; Truhlar, D. G. *J. Phys. Chem.* **1971**, *75*, 1844.

(3) (a) Fischer, H.; Radom, L. *Angew. Chem.* **2001**, *40*, 1340. (b) Last, I.; Baer, M. *J. Chem. Phys.* **1984**, *80*, 3246. (c) Cohen, N. *Int. J. Chem. Kinet.* **1982**, *14*, 1339.

(4) (a) Donahue, M. N.; Clarke, J. S.; Anderson, J. G. *J. Phys. Chem. A* **1998**, *102*, 3923. (b) Clarke, J. S.; Rypkema, H. A.; Kroll, J. H.; Donahue, M. N.; Anderson, J. G. *J. Phys. Chem. A* **2000**, *104*, 4458.

(5) Pross, A.; Yamataka, H.; Nagase, S. *J. Phys. Org. Chem.* **1991**, *4*, 135.

(6) Balint-Kurti, G. G.; Benneyworth, P. R.; Davis, M. J.; Williams, I. H. *J. Phys. Chem.* **1992**, *96*, 4346.

(7) (a) Salikhov, A.; Fischer, H. *Theor. Chim. Acta* **1997**, *96*, 114. (b) Harcourt, R. D. P.; Ng, R. *J. Phys. Chem.* **1993**, *97*, 12210.

(8) Fox, G. L.; Schlegel, H. B. *J. Phys. Chem.* **1992**, *96*, 298.

(9) Hrovat, D. A.; Borden, W. T. *J. Am. Chem. Soc.* **1994**, *116*, 6459.

(10) (a) Dunning, T. H. *J. Phys. Chem.* **1984**, *88*, 2469. (b) Dunning, T. H., Jr.; Harding, L. B.; Bair, R. A.; Eades, R. A.; Shepard, R. L. *J. Phys. Chem.* **1986**, *90*, 344.

(11) (a) Zavitsas, A. A. *J. Am. Chem. Soc.* **1972**, *94*, 2779. (b) Zavitsas, A. A.; Chatgillialoglu, C. *J. Am. Chem. Soc.* **1995**, *117*, 10654. (c) Zavitsas, A. A. *J. Am. Chem. Soc.* **1998**, *120*, 6578. (d) Blowers, P.; Masel, R. I. *J. Phys. Chem. A* **1999**, *103*, 7047; **1998**, *102*, 9957. (e) Johnston, H. S.; Parr, C. *J. Am. Chem. Soc.* **1963**, *85*, 2544.

(12) Roberts, B. P. *J. Chem. Soc., Perkin Trans. 2* **1996**, 2719.

(13) (a) Marcus, R. A. *Faraday Discuss. Chem. Soc.* **1960**, *29*, 21. (b) For a thorough evaluation in organic reactions, see; Eberson, L. *Electron-Transfer Reactions in OrganicChemistry*; Springer-Verlag: Berlin, 1987. (c) For a crticial assessment, see: Formosinho, S. J.; Arnaut, L. G.; Fausto, R. *Prog. Reaction Kinet.* **1998**, *23*, 1.

(14) (a) Lynch, B. J.; Fast, P. L.; Harris, M.; Truhlar, D. G. *J. Phys. Chem. A* **2000**, *104*, 4812. (b) Garrett, B. C.; Truhlar, D. G.; Wagner, A. F.; Dunning, T. H., Jr. *J. Chem. Phys.* **1983**, *78*, 4400.

(15) See for example, Dubey, M. K.; Morschladt, R.; Donahue, N. M.; Anderson, J. G. *J. Phys. Chem. A* **1997**, *101*, 1494.

(16) (a) Shaik, S.; Hiberty, P. C. In *Theoretical Models for Chemical Bonding*; Maksic, Z. B., Ed.; Springer-Verlag: Heidelberg, 1991; Vol. 4, p 269. (b) Shaik, S.; Shurki, A. *Angew. Chem., Int. Ed. Engl.* **1999**, *38*, 586. (c) Shaik, S. S. *J. Am. Chem. Soc.* **1981**, *103*, 3692.

(17) (a) Shaik, S.; Wu, W.; Dong, K.; Song, L.; Hiberty, P. C. *J. Phys. Chem. A* **2001**, *105*, 8226. (b) Maitre, P.; Hiberty, P. C.; Ohanessian, G.; Shaik, S. *J. Phys. Chem.* **1990**, *94*, 4089.

(18) (a) Hiberty, P. C.; Flament, J. P.; Noizet, E. *Chem. Phys. Lett.* **1992**, *189*, 259. (b) Hiberty, P. C.; Humbel, S.; Byrman, C. P.; Van Lenthe, J. H. *J. Chem. Phys.* **1994**, *101*, 5969. (c) Hiberty, P. C.; Humbel, S.; Archirel, P. *J. Phys. Chem.* **1994**, *98*, 11697. (d) Hiberty, P. C. In *Modern Electronic Structure Theory and Applications in Organic Chemistry*; Davidson, E. R., Ed.; Word Scientific: River Edge, NY, 1997; pp 289−367. (e) Hiberty, P. C.; Shaik, S. In *Valence Bond Theory*, Cooper, D. L., Ed.; Elsevier: Amsterdam, 2002; pp 187−225. (f) Hiberty, P. C.; Shaik, S. *Theor. Chem. Acc.*, in press.

(19) (a) Wu, W.; Song, L.; Cao, Z.; Zhang, Q.; Shaik, S. *J. Phys. Chem. A* **2002**, *106*, 2721. (b) Cooper, D. L.; Gerratt, J.; Raimondi, M. *Adv. Chem. Phys.* **1987**, *69*, 319. (c) Clarke, N. J.; Raimondi, M.; Sironi, M.; Gerratt, J.; Cooper, D. L. *Theor. Chem. Acc.* **1998**, *99*, 8.

(20) (a) Goddard, W. A., III; Harding, L. B. *Annu. Rev. Phys. Chem.* **1978**, *29*, 363. (b) Cooper, D. L.; Gerratt, J.; Raimondi, M. *Chem. Rev.* **1991**, *91*, 929.

(21) (a) Wu, W.; Shaik, S. *Chem. Phys. Lett.* **1999**, *301*, 37. (b) Mcweeny, R. *Int. J. Quantum Chem.* **1999**, *74*, 87.

(22) (a) Shaik, S.; Hiberty, P. C. *Adv. Quantum Chem.* **1995**, *26*, 99. (b) Shaik, S.; Schlegel, H. B.; Wolfe, S. *Theoretical Aspects of Physical Organic Chemistry. The $S_N2$ Mechanism*; Wiley: New York, 1992. (c) Shaik, S. S. *Prog. Phys Org. Chem.* **1985**, *15*, 197. (d) Pross, A. *Theoretical and Physical Principles of Organic Reactivity*; John Wiley & Sons: New York, 1995; pp 113−121.

(23) Mayo, F. R.; Walling, C. *Chem. Rev.* **1950**, *46*, 191.

(24) Chirgwin, H. B.; Coulson, C. A. *Proc. R. Soc. London, Ser. A* **1950**, *2*, 196.

(25) (a) Hay, P. J.; Wadt, W. R. *J. Chem. Phys.* **1985**, *82*, 270. (b) Petersson, G. A.; Al-Laham, M. A. *J. Chem. Phys.* **1991**, *94*, 6081.

(26) Gonzalez, C.; Schlegel, H. B. *J. Chem. Phys.* **1989**, *90*, 2154.

(27) (a) Shaik, S.; Ioffe, A.; Reddy, A. C.; Pross, A. *J. Am. Chem. Soc.* **1994**, *116*, 262. (b) Shaik, S.; Reddy, C. A. *J. Chem. Soc., Faraday Trans.* **1994**, *90*, 1631. (c) Note that the perfectly resonating state (PRS) and ACS are not the same states. For PRS see, Shurki, A.; Shaik, S. *J. Mol. Struct. (THEOCHEM)* **1998**, *424*, 37.

(28) Wu, W.; Song, L.; Mo, Y.; Zhang, Q. XIAMEN99−An Ab Initio Spin-free Valence Bond Program, Xiamen University, Xiamen, 1999.

(29) Frisch, M. J.; Trucks, G. W.; Schlegel, H. B.; Scuseria, G. E.; Robb, M. A.; Cheeseman, J. R.; Zakrzewski, V. G.; Montgomery, J. A., Jr.; Stratmann, R. E.; Burant, J. C.; Dapprich, S.; Millam, J. M.; Daniels, A. D.; Kudin, K. N.; Strain, M. C.; Farkas, O.; Tomasi, J.; Barone, V.; Cossi, M.; Cammi, R.; Mennucci, B.; Pomelli, C.; Adamo, C.; Clifford, S.; Ochterski, J.; Petersson, G. A.; Ayala, P. Y.; Cui, Q.; Morokuma, K.; Malick, D. K.; Rabuck, A. D.; Raghavachari, K.; Foresman, J. B.; Cioslowski, J.; Ortiz, J. V.; Baboul, A. G.; Stefanov, B. B.; Liu, G.; Liashenko, A.; Piskorz, P.; Komaromi, I.; Gomperts, R.; Martin, R. L.; Fox, D. J.; Keith, T.; Al-Laham, M. A.; Peng, C. Y.; Nanayakkara, A.; Challacombe, M.; Gill, P. M. W.; Johnson, B.; Chen, W.; Wong, M. W.; Andres, J. L.; Gonzalez, C.; Head-Gordon, M.; Replogle, E. S.; Pople, J. A. *Gaussian 98*, Gaussian, Inc.: Pittsburgh, PA, 1998.

(30) Heitler, W.; London, F. *Z. Physik* **1927**, *44*, 455.

(31) Hammond, G. S. *J. Am. Chem. Soc.* **1955**, *77*, 334.

(32) Shaik, S.; Duzy, E.; Bartuv, A. *J. Phys. Chem.* **1990**, *94*, 6574.

(33) (a) Wu, W.; Danovich, D.; Shurki, A.; Shaik, S. *J. Phys. Chem. A* **2000**, *104*, 8744. (b) Shaik, S.; de Visser, S. P.; Wu, W.; Song, L.; Hiberty, P. C. *J. Phys. Chem. A* **2002**, *106*, 5043.

(34) Malrieu, J. P. *Nouv. J. Chim.* **1986**, *10*, 61.